

Characterization and application of surface-molecular-imprinted-polymer modified TiO₂ nanotubes for removal of perfluorinated chemicals

Lei Hu, Yi Li and Wenlong Zhang

ABSTRACT

The removal of perfluorinated chemicals (PFCs) during wastewater reclamation is a great concern. However, the existing advanced treatment processes are inefficient for the removal of PFCs from secondary effluents of municipal wastewater treatment plants (WWTPs) because other coexistent pollutants with less environmental significance are removed simultaneously. Therefore, research on high-selectivity, low-cost removal methods is needed. The S-MIP-TiO₂ nanotube (NT) photocatalysts were fabricated, characterized and tested for removal of PFCs from wastewater for the first time. Scanning electron microscopy and Fourier transform infrared spectroscopy show that the TiO₂ NTs (average diameter 60 nm) were successfully imprinted with functional groups (i.e. carboxyl). The adsorption selectivity and photocatalytic activity of the S-MIP-TiO₂ NTs over perfluorooctanoic acid (PFOA) were improved compared with neat TiO₂ NTs and interestingly, were higher at low PFOA concentrations (10 to 100 ng/L, as normal PFC concentrations in secondary effluents) than at high concentrations (10 to 1,000 mg/L). With S-MIP-TiO₂ NTs used as photocatalysts, some representative PFCs were selectively and rapidly removed from secondary effluents of a municipal WWTP. S-MIP-TiO₂ NTs exhibited excellent regeneration performance. Thus, photocatalytic treatment using is promising for effective removal of PFCs from secondary effluents of municipal WWTPs.

Key words | perfluorinated chemicals, removal, surface-molecular-imprinting, TiO₂ nanotubes

Lei Hu

Yi Li (corresponding author)

Wenlong Zhang

Key Laboratory of Integrated Regulation and Resource Development on Shallow Lakes, Ministry of Education, College of Environment, Hohai University, Xikang Road #1, Nanjing 210098, China
E-mail: 10236551@qq.com

INTRODUCTION

In recent years, wastewater reclamation from municipal wastewater treatment plants (WWTPs) has been employed worldwide for various purposes, including landscape irrigation, impoundment, crop irrigation, and groundwater recharge to overdrawn aquifers (Zhang *et al.* 2011). However, many types of pollutants still exist in the effluents of municipal WWTPs after traditional treatment (Gupta *et al.* 2011b, 2012a). Among them, perfluorinated chemicals (PFCs) are at mean concentrations from ng/L to µg/L. Some PFCs, such as perfluorinated acid, are included in the European Union list of priority pollutants. These chemicals even at trace levels can induce extensive reproductive and sexual abnormalities in wildlife (Radjenovic *et al.* 2007). Thus, the removal of these PFCs during wastewater reclamation is a great concern.

Many methods, such as activated carbon adsorption, ozonation, UV radiation, UV/H₂O₂ degradation, and

photo-degradation, have been developed to remove PFCs from wastewater (Zhang *et al.* 2012). Among them, activated carbon has been widely applied to remove organic matters from wastewater owing to its strong affinity to adsorb even low-concentration organic substances (Ali & Gupta 2006; Gupta *et al.* 2006, 2007; Gupta & Ali 2008; Gupta *et al.* 2011a). Photo-degradation is an environmentally friendly technique since it does not require chemical input or output (Gupta *et al.* 2007, 2011b, 2012b). TiO₂ is the most common photocatalyst due to its capability in removal of a wide range of pollutants, and shows other advantages including high photochemical stability, low toxicity and low-cost (Gupta *et al.* 2011a, 2012a).

However, the presence of low-level PFCs is accompanied by high levels of other low-toxicity biodegradable pollutants in secondary effluents of municipal WWTPs (Saadi *et al.* 2006). Current advanced treatment processes

are inefficient for PFCs removal because other pollutants with less environmental significance were also removed simultaneously, which decreases the removal efficiency of PFCs and increases treatment costs (Czili & Horvath 2008). For these reasons, the research for highly selective and low-cost removal methods is still warranted.

Molecular imprinting is a useful technique for the preparation of polymeric materials as specific molecular recognition receptors (Piletsky *et al.* 2001; Haupt 2003). Molecularly imprinted polymers (MIPs) are prepared by copolymerization of a cross-linking agent with the complex formed from a template and polymerizable monomers that have functional groups specifically interacting with the template through covalent or non-covalent bonds. After the template is removed from the resulting polymer matrixes, binding sites having the size and shape complementary to the template are generated. These MIPs are synthesized with 'tailor-made' binding sites for a template (Haupt 2003). Recently, MIPs have been utilized for the selective removal of perfluorinated compounds from water (Meng *et al.* 2005; Le Noir *et al.* 2007; Zhang *et al.* 2011). Meng *et al.* (2005) suggested that MIPs with perfluorinated acid as template might be used to remove perfluorinated compounds from water. Le Noir *et al.* (2007) employed MIPs, based on bulk polymerization approach, to remove trace perfluorinated acid from aqueous solution using MIPs adsorbent column. Tran *et al.* (2014) used molecularly imprinted polymeric microspheres to remove phenolic estrogen pollutants from different sources of water. The results of the above studies show that MIPs adsorption is an effective method for the selective removal of trace targeted perfluorinated compounds from water.

However, adsorption is a non-destructive removal technology and MIPs need to be regenerated and reused for a lower treatment cost (Sansotera *et al.* 2014). The related research concerning simultaneous adsorption of perfluorinated compounds and polymer regeneration are very limited. Only recently, UV irradiation was used as a method to regenerate MIPs and destroy pollutants during solvent extraction (Jing *et al.* 2014). It has been reported in our previous research that TiO₂ photocatalysis is more effective for the removal of perfluorinated compounds and perfluorinated activity from secondary effluents than UV irradiation (Zhang *et al.* 2012). However, to the best of our knowledge, there is no existing report regarding the selective removal of perfluorinated compounds using the technology combining of MIPs adsorption and TiO₂ photocatalysis.

The main objective of this work was, therefore, to develop new surface-MIP-modified TiO₂ (S-MIP-TiO₂) nanotube (NT)

photocatalysts to achieve selective removal of perfluorinated compounds from secondary effluents and simultaneous regeneration of polymers. The material characteristics, adsorption properties, and photocatalytic activity of the photocatalysts were investigated in details. The photocatalytic removal of PFCs and perfluorinated activity from practical secondary effluent using S-MIP-TiO₂ NTs were also evaluated.

MATERIAL AND METHODS

Reagents

The titanium sheets (99.60%, 0.06 mm thick) were purchased from Haiji Ltd for Titanium & Nickel, China. The five perfluorinated compounds [heptafluorobutyric acid (PFBA), perfluorovaleric acid (PFPeA), undecafluorohexanoic acid (PFHxA), perfluoroheptanoic acid (PFHpA), and pentafluorooctanoic acid (PFOA)], methacrylic acid (MAA), trimethylolpropane trimethacrylate (TRIM), and 4,4'-azobis(4-cyanovaleric acid) (AIBN) were all purchased from Sigma-Aldrich (USA) and used without further purification. TRIM was of technical grade and all other reagents used were of high-performance liquid chromatography (HPLC) grade. Analytical standards for chromatography analyses were purchased from Sigma-Aldrich (USA).

Preparation of TiO₂ NTs and S-MIP-TiO₂ NTs

TiO₂ NTs were prepared according to previous work (Su *et al.* 2009). Prior to anodization, titanium sheets were ultrasonically cleaned in acetone and deionized water. The cleaned titanium sheet was anodized at 20 V in an electrolyte containing 0.5 wt% NH₄F and 1/12 M C₂H₂O₄·2H₂O at room temperature for 10 min in a two-electrode system with a nickel cathode. To induce crystallinity, the initially amorphous as-anodized sample was annealed at 500 °C for 120 min with heating and cooling rates of 2 °C·min⁻¹.

The MIP was prepared by precipitation polymerization method. The template (PFOA, 0.18 mmol) was first added into a bottle containing a mixture of solvent (anhydrous acetonitrile, 10 mL) and functional monomer (MAA, 0.87 mmol), and sonicated for 5 min at ambient temperature. The cross-linker (TRIM, 1.90 mmol) and initiator (AIBN, 0.0071 mmol) were then added into the solution. The solution was mixed uniformly by sonication for 5 min, and then was slowly dropped on two sides of TiO₂ NTs to get a uniform coating. Afterwards, the coated-TiO₂ NTs were fixed in the columniform quartz tube. The tube was

then sealed and purged with nitrogen for a further 20 min. Polymerization was carried out under UV light irradiation for 12 h. Then the coated-TiO₂ NTs were washed with a mixture of methanol and acetic acid (volume ratio of 9:1) for four times, and each at a duration of 1.5 h. Then, the nanotube array was washed with methanol for 24 h. This was followed by extractions with methanol until no PFOA was detected in the eluates. The non-imprinted polymer (NIP) modified TiO₂ nanotubes were synthesized and treated in the same way except that no template was added.

Characterization

The morphological characters of the samples were investigated using field emission scanning electron microscope (Hitachi, Model S-4800). The completion of the reaction in the preparation of the MIPs modified NTs was demonstrated by FD-5DX Fourier transform infrared spectroscopy (FT-IR). The crystal phases were determined by X-ray diffractometer (XRD, M21X, MAC Science Ltd, Japan) with Cu-K_α radiation.

Apparatus and methods for adsorption and photocatalytic degradation

The adsorption of PFOA on MIP-TiO₂ NTs, NIP-TiO₂ NTs and TiO₂ NTs were performed by placing these samples in the solutions (300 mL) at different concentrations of PFOA (varied from 10 to 10⁹ ng/L). The whole process went on with continuous magnetic stirring for 2 h in the dark at room temperature. The amount of adsorbed PFOA was determined by measuring the difference between total PFOA amount and residual amount in solution.

The photocatalytic experiments were conducted in a water-jacketed cylindrical quartz photocatalytic reactor (60 cm height, 18 cm outer diameter, and 15 cm inner diameter) in the presence of the photocatalysts with the active area 400 cm²/L. The double-walled glass reservoir was equipped with a thermostatically controlled water flow between the outer walls. The aeration system at the bottom of the reactor was installed to improve mixing and mass transfer to the catalyst. An 8 W, low-pressure mercury UV lamp (Beijing Lighting Research Institute, ZW8S15W) with irradiating wavelength 254 nm as the light source was immersed in the photocatalytic reactor. Under the same conditions as in the photocatalytic experiments, the total useful radiation arriving to the reactor was determined to be 7.38×10^{-8} Einstein·s⁻¹ by chemical actinometry using potassium ferrioxalate (Sun & Bolton 1996). After the

solution was stirred for 40 min to favor the organic adsorption onto the catalyst surface, the concentration of the pollutant was determined as the initial concentration, and then the irradiation started. The solution was sampled for analysis from the reactor cell using a glass syringe at specified time intervals during degradation.

Analytical methods

The concentrations of PFOA in ultrapure water were determined using liquid chromatography–mass spectrometry (LC-MS) equipped with electrospray interface (HP 1100 LC-MS_n Trap SL System, Agilent, USA) in negative ionization mode for isolation of m/z 271 ([M-H]⁻ ion). During the process, the mobile-phase composition was methanol/water 75/25 (v/v) at a flow rate of 0.18 mL·min⁻¹. Stop time was set to be 6 min.

To determine the PFCs in secondary effluents, solid phase extraction (SPE) method was applied to concentrate the compounds from the wastewater sample using Oasis HLB resin cartridges (Waters Corporation, USA) previously washed with 10 mL of ethyl acetate, 10 mL methanol, and 15 mL ultrapure water. The dried eluate post SPE were derived with 100 μL pyridine and 50 μL *N,O*-bis(trimethylsilyl) trifluoroacetamide solution containing 1% trimethylchlorosilane (Sigma) at 70 °C for 60 min, followed by cooling down to room temperature.

RESULTS AND DISCUSSION

Characterization of as-prepared photocatalyst

The surface morphologies of TiO₂ NTs and S-MIP-TiO₂ NTs are shown in Figure 1. Neat TiO₂ NTs (Figure 1(a)) were composed of well-ordered and uniform TiO₂ nanotubes, with pore sizes ranging from 55 to 75 nm, and the average pore size of approximately 60 nm, and a wall thickness of approximately 14 nm. Most S-MIP-TiO₂ NTs (Figure 1(b)) were still open at the top end, similar with the TiO₂ NTs. In the process of MIP modification, the mixture was supposed to diffuse down the length of the hollow core of the NTs. Hence, the inside surface of the NTs was modified with a thin MIP layer, decreasing the average diameter from approximately 60 to 50 nm.

Compared with TiO₂ NTs (Figure 2(a)), the IR spectrum of the TiO₂ NTs with a PFOA-imprinted layer (Figure 2(b)) had the characteristic peaks of PFOA at 3,446, 3,240, 2,930, 2,864, 1,590, and 1,250 cm⁻¹ (Cakmak *et al.* 2006), and the characteristic peaks of MAA at 1,650 and 1,820 cm⁻¹

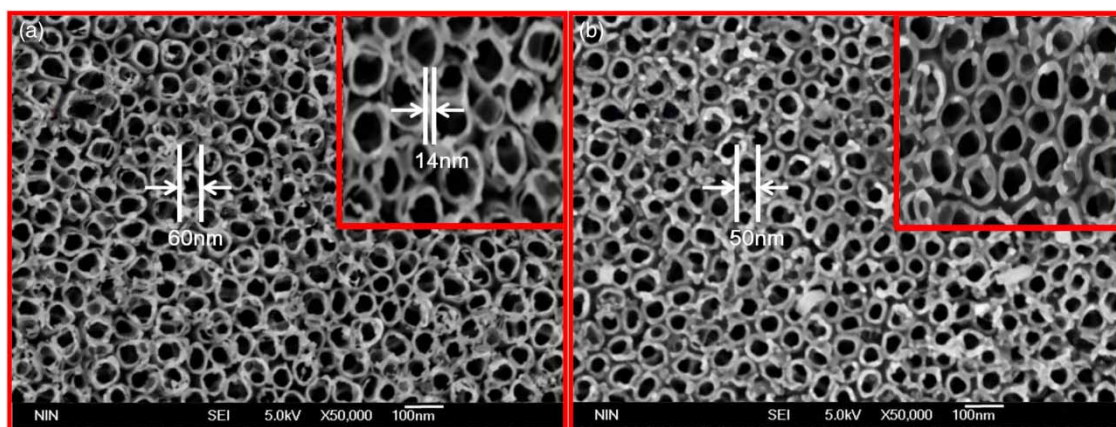


Figure 1 | Surface-view SEM images of: (a) TiO₂ NTs, (b) S-MIPs-TiO₂ NTs.

(Martínez *et al.* 2008). After removing PFOA using methanol and acetic acid, the characteristic peaks assigned to PFOA disappeared. In contrast, the characteristic peaks assigned to MAA were still clearly observed (Figure 2(c)). This result indicated that the functional monomer of the target molecule PFOA was successfully imprinted on the surface of TiO₂ NT.

Both the XRD spectra of the neat TiO₂ NTs (Figure 3(a)) and S-MIP-TiO₂ NTs (Figure 3(b)) exhibited clear characteristic diffraction peaks at 25.34°, 37.84°, 48.02°, 53.00°, 55.02°, 62.86°, 70.58°, and 76.24°, which were assigned to the anatase phase. The XRD patterns revealed the crystallization of TiO₂ NTs was not affected by the surface molecular imprinted process.

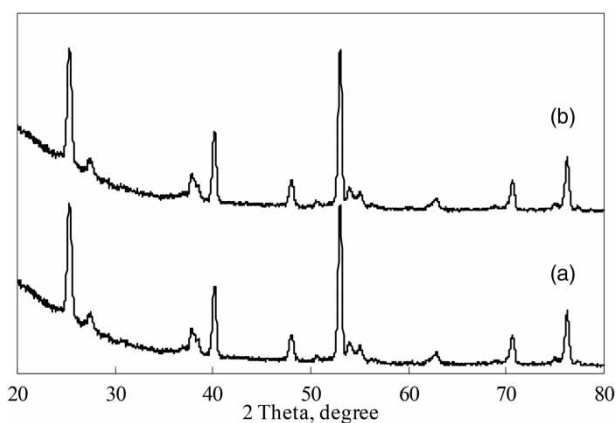


Figure 3 | XRD patterns of (a) TiO₂ NTs, (b) S-MIPs-TiO₂ NTs.

Adsorption of the template molecules

The adsorption of the template compounds PFOA on S-MIP-TiO₂ NTs, NIP-TiO₂ NTs, and TiO₂ NTs are shown

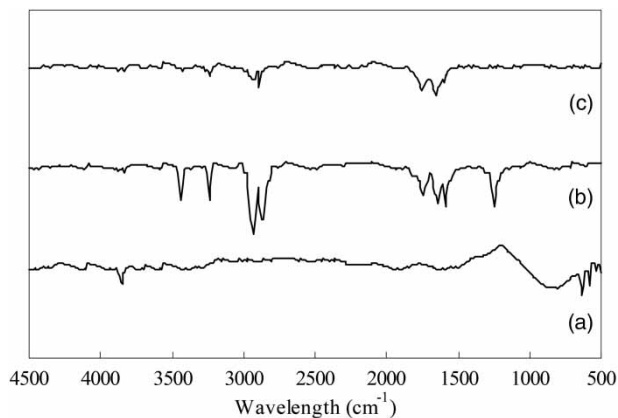


Figure 2 | FT-IR spectra of (a) TiO₂ NTs, (b) S-MIPs-TiO₂ NTs before being treated with methanol and acetic acid, (c) S-MIPs-TiO₂ NTs.

in Figure 4. The adsorption isotherms were described by the Freundlich isotherm model ($Q_e = K_f C_e^{1/n}$). In this model, Q_e is the amount of PFOA adsorbed per unit active surface area of the photocatalysts ($\text{mg}\cdot\text{cm}^{-2}$), C_e is the concentration of PFOA in solution ($\text{ng}\cdot\text{L}^{-1}$), K_f is the adsorption equilibrium constant representative of the adsorption capacity, and $1/n$ is a constant indicative of the adsorption intensity. The values of the parameters are listed in Table 1. In the investigated concentration range, $1/n$ of the S-MIP-TiO₂ NTs (0.2711) was higher than that of the NIP-TiO₂ NTs (0.1754) and TiO₂ NTs (0.1187). K_f of the S-MIP-TiO₂ NTs was 3.89, higher than those for NIP-TiO₂ NTs and TiO₂ NTs (2.04 and 1.65, respectively). These results indicated that the adsorption capacity and intensity of both S-MIP-TiO₂ NTs and NIP-TiO₂ NTs were enhanced during the precipitation polymerization process. The S-MIP-TiO₂ NTs had the highest adsorption capacity and intensity among the three photocatalysts.

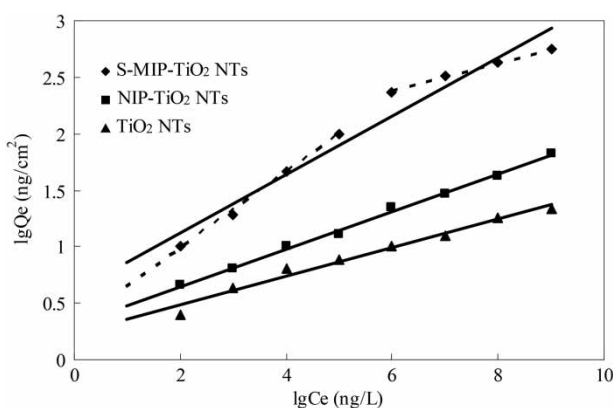


Figure 4 | Adsorption isotherms of S-MIP-TiO₂ NTs, NIP-TiO₂ NTs, and TiO₂ NTs for PFOA in ultrapure water.

According to the adsorption isotherms, an adsorption hypothesis involving three types of potential binding sites on the surface of the modified photocatalyst was proposed as shown in Figure 5. For binding site type 1, only the template molecules could be bound theoretically because the binding sites require not only specific functional groups, but also matching target molecule sizes. Binding site type 2 could occur both specific by specific functional group recognition and non-specific adsorption via hydrogen bonding. Binding site type 3 could occur non-specific adsorption via hydrogen bonding. After polymerization, some functional monomers that do not form complexes could remain on the surface of the polymer. These monomers provide the possibility of non-specific adsorption via hydrogen bonding. Three types of potential binding sites could be formed on the surface of S-MIP-TiO₂ NTs, and one type (type 3) on the surface of the NIP-TiO₂ NTs.

In general, the Freundlich model is suitable for assessing the adsorption isotherm of S-MIP-TiO₂ NTs. However, in the current study, the Freundlich model yielded a worse fit for the adsorption isotherm of PFOA on S-MIP-TiO₂ NTs ($R^2 = 0.9361$) than in previous studies ($R^2 \geq 0.99$) (Zhang *et al.* 2008). This discrepancy can be explained by the fact that

the investigated adsorption concentration range (from 10 ng/L to 1,000 mg/L) was much wider than those in previous studies (from 1 to 1,000 mg/L) (Zhang & Hu 2008). The adsorption isotherms of PFOA on S-MIP-TiO₂ NTs are shown in Figure 4. It could be found that the Freundlich model constant $1/n$ at low concentrations of PFOA (from 10 to 10⁵ ng/L) was higher than that at high concentrations (from 10⁶ to 10⁹ ng/L). It indicated that the adsorption intensity of PFOA on S-MIP-TiO₂ NTs at low concentrations (from 10 to 10⁵ ng/L) was higher than that at high concentrations (from 10⁶ to 10⁹ ng/L). According to the adsorption hypothesis proposed in this study, the adsorption of template compounds on the S-MIP-TiO₂ NTs had two different adsorption mechanisms, i.e. functional group recognition and interaction between π electrons. The attractive force of functional group recognition between carboxyl and phenolic hydroxyl is stronger than the interaction force between π electrons in the phenol aromatic ring and in the cross-linker (Wang *et al.* 2006; An *et al.* 2008; Alizadeh & Akhondian 2010). Therefore, the adsorption of low concentration PFOA on S-MIP-TiO₂ NTs most resulted from functional group recognition (potential binding sites 1 and 2). In contrast, the weak interaction forces (potential binding site 3) were the major adsorption mechanism at high concentrations of PFOA. It can be deduced that the functional group recognition exhibited higher adsorption intensity towards the template molecules than weak interaction.

Photocatalytic removal of the template molecules

The photocatalytic degradation activities of the S-MIP-TiO₂ NTs, NIP-TiO₂ NTs, and TiO₂ NTs were evaluated in an aqueous PFOA solution. The photocatalytic reaction kinetics followed the Langmuir-Hinshelwood model (Zhang *et al.* 2011).

$$r = \frac{dC}{dt} = \frac{kKC}{1 + KC} \quad (1)$$

Table 1 | Freundlich isotherm parameters for adsorption PFOA

Photocatalysts	Initial concentration (ng/L)						K_f
	[10, 10 ⁵]		[10 ⁶ , 10 ⁹]		[10, 10 ⁹]		
	1/n	R^2	1/n	R^2	1/n	R^2	
S-MIP-TiO ₂ NTs	0.3381	0.9969	0.1253	0.9938	0.2711	0.9316	3.89
NIP-TiO ₂ NTs	–	–	–	–	0.1754	0.9969	2.04
TiO ₂ NTs	–	–	–	–	0.1187	0.9985	1.65

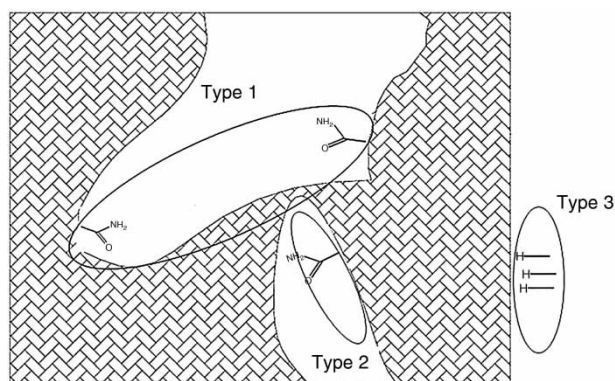


Figure 5 | Three potential binding sites on the surface of the modified photocatalyst.

where C is the PFOA concentration, k is the degradation rate constant, and K is the adsorption equilibrium constant. In the current study, the PFOA concentration C was less than $1 \times 10^{-3} \text{ mol}\cdot\text{L}^{-1}$, which made $KC < 1$. Hence, Equation (1) can be transformed into:

$$r = \frac{dC}{dt} = kKC = k_{app}C \quad (2)$$

The integration of Equation (2) would lead to the expected relationship:

$$\ln\left(\frac{C_0}{C}\right) = k_{app}t \quad (3)$$

$$k_{app} = kK \quad (4)$$

where C_0 and C are the concentrations of PFOA at the beginning and at time t , respectively, and k_{app} is the apparent degradation rate constant. PFOA degradation in the UV irradiation experiments also followed a pseudo-first-order kinetics (Sansotera et al. 2014). As shown in Figure 6, the apparent first-order rate constant k_{app} in a different process can be easily calculated: 0.0040 min^{-1} in the photolysis process, 0.0225 min^{-1} for the TiO_2 NTs, 0.0316 min^{-1} for the NIP- TiO_2 NTs, and 0.0732 for the S-MIP- TiO_2 NTs in the photocatalytic process, respectively. These results indicated that TiO_2 photocatalysis was more efficient than direct photolysis for PFOA removal, and the photocatalytic degradation process was enhanced with the presence of the MIP layer.

In this process, the photocatalytic reaction started with the adsorption of the template compound molecules PFOA on the MIPs layers located on the surface TiO_2 NTs. Then the adsorbed PFOA molecules were oxidized by the generated $\cdot\text{OH}$ radicals during photocatalysis.

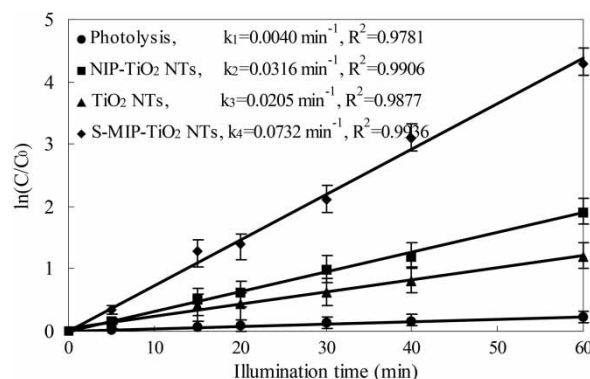


Figure 6 | Kinetic data for direct photolysis and photocatalytic degradation of PFOA over S-MIP- TiO_2 NTs, NIP- TiO_2 NTs, and TiO_2 NTs. The initial concentration of PFOA was $10 \mu\text{g/L}$.

Therefore, the photocatalytic degradation rate strongly depended on the amount of PFOA adsorbed on the photocatalyst surface, and on the amount of $\cdot\text{OH}$ generated during photocatalysis, as shown in Equation (4). It has been confirmed that the adsorption capacity and intensity of PFOA on S-MIP- TiO_2 NTs was higher than TiO_2 NTs, although the incident light would be hindered by MIPs layer on the surface of TiO_2 NTs, and thus hinder the $\cdot\text{OH}$ generation during S-MIP- TiO_2 photocatalysis (Liu et al. 2010). Therefore, the enhanced photocatalytic degradation should result from the enhanced adsorption capacity and intensity despite the negative effects of MIPs layer.

The effect of concentration on the photocatalytic degradation rate of PFOA was also investigated. As shown in Figure 7, when the initial PFOA concentration increased from 10^2 ng/L to 10^9 ng/L , k_{app} of PFOA degradation decreased from 0.784 to 0.071 min^{-1} using the S-MIP- TiO_2 NTs, and from 0.109 to 0.029 min^{-1} using the TiO_2 NTs. The ratio of the k values using S-MIP- TiO_2 NTs to TiO_2 NTs was decreased from 7.19 to 2.45. The result indicated

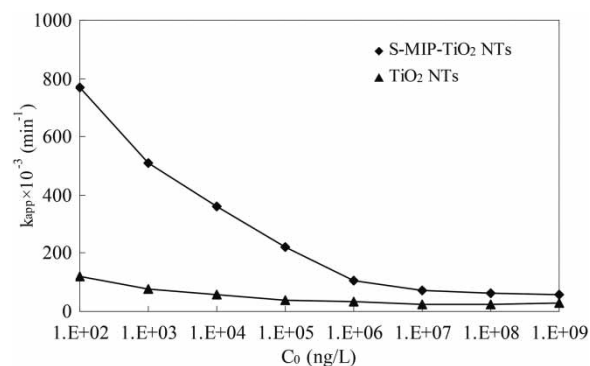


Figure 7 | Initial concentration dependence of the degradation rate constant of PFOA over the corresponding S-MIP- TiO_2 NTs and TiO_2 NTs.

that the degradation selectivity of S-MIP-TiO₂ NTs towards the template compounds (PFOA) was increased as the initial concentration of PFOA was decreased, which would be helpful for the selective removal of the low-level template compounds in wastewater.

Based on the above analysis, the S-MIP-TiO₂ NTs not only exhibited outstanding adsorption capacity and photocatalytic activity toward the template compounds, but also had higher adsorption intensity and photocatalytic selectivity at low concentrations than that at high concentrations. Therefore, photocatalytic treatment using S-MIP-TiO₂ NT as photocatalysts may be a promising approach for the removal of trace perfluorinated compounds from secondary effluents.

Photocatalytic removal of PFCs

The feasibility of applying S-MIP-TiO₂ NTs for the selective removal of perfluorinated compounds from wastewater was evaluated by investigating the photocatalytic removal efficiency of five perfluorinated compounds (PFBA, PFPeA, PFOA, PFHxA, and PFHpA) from the secondary effluents of a municipal WWTP as shown in Figure 8. The initial concentration of five PFCs was 10 µg/L. These compounds were chosen as the representative chemicals to be detected in the secondary effluents because of their wide occurrence and high potential toxicity.

It is known that the photocatalytic degradation process can be divided into two stages, i.e. adsorption and photocatalytic degradation phases. In adsorption phase (0–40 min), the functional group recognition was the major adsorption mechanism because the concentrations of PFCs in secondary effluent range from ng/L to µg/L. As shown in previous work, the functional group recognition is the chemical interaction between the functional groups (–OH)

in target molecules and the footprints groups (carboxyl) in polymer. Therefore, the compounds comprising the functional groups in their molecules (such as PFBA, PFPeA, PFHxA, and PFHpA) were chemically adsorbed on the surface of S-MIP-TiO₂ NTs, resulting in an enhanced photocatalytic degradation and a rapid removal of PFCs. In comparison, the compounds without these functional groups were not enhanced adsorbed and degraded during the same process.

The pH value of the solution is an important parameter, which affects the adsorption behavior of the ion in many cases. The adsorbent surface was charged through the protonation of functional groups and the electrostatic attraction between adsorbents and adsorbates usually plays a major role. It can be found that the adsorption is pH dependent, and the adsorption amount of PFOA decreased with increasing solution pH value. Therefore, the electrostatic interaction played an important role in the sorption process at acidic pH values. With increasing solution pH, the adsorption amount of the MIPs and NIPs adsorbents for PFOA decreased. It indicated that the adsorption of PFOA onto the MIPs and NIPs adsorbents was mainly attributed to the electrostatic attraction. Other forces including hydrophobic interaction and hydrogen binding may be involved in the adsorption in the whole pH range, but their contributions are limited in this study. It also can be found that the MIPs adsorbents had higher sorption capacity than that of the NIPs adsorbents at pH values from 4 to 6, showing the good selective adsorption. The initial pH value of the solution is 5 in this work.

The S-MIP-TiO₂ NTs were also reused to test its stability for the removal of perfluorinated activity from the secondary effluents. It was found that the removal efficiency was slightly reduced after each use and finally stable at about 82% after five cycles. The result indicates that photocatalytic treatment using S-MIP-TiO₂ NTs could be a promising approach for effectively eliminating PFCs from secondary effluents of municipal WWTPs.

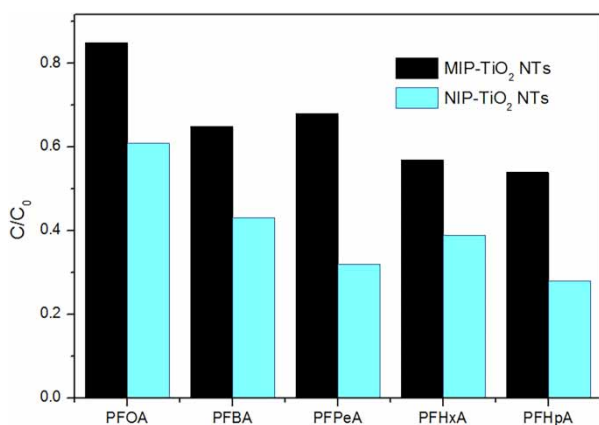


Figure 8 | The removal efficiency of five kinds PFCs.

CONCLUSIONS

Surface-molecular-imprinted polymer-modified TiO₂ nanotube (S-MIP-TiO₂ NT) photocatalysts were prepared. The MIP layer provided the neat TiO₂ NTs with selective molecular adsorption ability, leading to outstanding adsorption capacity and intensity and enhanced photocatalytic selectivity and activity over PFOA. Moreover, the modified photocatalysts exhibit higher adsorption intensity and

photocatalytic selectivity at low concentrations than at high concentrations.

The photocatalytic removal of PFCs and perfluorinated activity from secondary effluents of a municipal WWTP was considerably enhanced using S-MIP-TiO₂ NTs than using TiO₂ NTs. The S-MIP-TiO₂ NTs developed here also exhibit excellent regeneration performance. Therefore, photocatalytic treatment with S-MIP-TiO₂ NTs could be a promising approach for effective elimination of PFCs from secondary effluents of municipal WWTPs. This method would help to reduce ecological risk during wastewater reclamation.

ACKNOWLEDGEMENTS

This study was funded by National Natural Science Foundation of China (No. 51009050) and the Priority Academic Program Development of Jiangsu Higher Education Institutions (PAPD).

REFERENCES

- Ali, I. & Gupta, V. K. 2006 *Advances in water treatment by adsorption technology*. *Nat. Protoc.* **1** (6), 2661–2667.
- Alizadeh, T. & Akhoundian, M. 2010 *A novel potentiometric sensor for promethazine based on a molecularly imprinted polymer (MIP): the role of MIP structure on the sensor performance*. *Electrochimica Acta* **55** (10), 3477–3485.
- An, F. Q., Gao, B. J. & Feng, X. Q. 2008 *Adsorption and recognizing ability of molecular imprinted polymer MIP-PEI/SiO₂ towards phenol*. *Journal of Hazardous Materials* **157** (2–3), 286–292.
- Cakmak, G., Togan, I. & Severcan, F. 2006 *17 beta-estradiol induced compositional, structural and functional changes in rainbow trout liver, revealed by FT-IR spectroscopy: A comparative study with nonylphenol*. *Aquatic Toxicology* **77** (1), 53–63.
- Czili, H. & Horvath, A. 2008 *Applicability of coumarin for detecting and measuring hydroxyl radicals generated by photoexcitation of TiO₂ nanoparticles*. *Applied Catalysis B-Environmental* **81** (3–4), 295–302.
- Gupta, V. K. & Ali, I. 2008 *Removal of endosulfan and methoxychlor from water on carbon slurry*. *Environmental Science & Technology* **42** (3), 766–770.
- Gupta, V. K., Mittal, A., Gajbe, V. & Mittal, J. 2006 *Removal and recovery of the hazardous azo dye acid orange 7 through adsorption over waste materials: bottom ash and de-oiled soya*. *Industrial & Engineering Chemistry Research* **45** (4), 1446–1453.
- Gupta, V. K., Jain, R., Mittal, A., Mathur, M. & Sikarwar, S. 2007 *Photochemical degradation of the hazardous dye Safranin-T using TiO₂ catalyst*. *Journal of Colloid and Interface Science* **309** (2), 464–469.
- Gupta, V. K., Jain, R., Agarwal, S. & Shrivastava, M. 2011a *Kinetics of photo-catalytic degradation of hazardous dye Tropaeoline 000 using UV/TiO₂ in a UV reactor*. *Colloids and Surfaces A-Physicochemical and Engineering Aspects* **378** (1–3), 22–26.
- Gupta, V. K., Jain, R., Nayak, A., Agarwal, S. & Shrivastava, M. 2011b *Removal of the hazardous dye-Tartrazine by photodegradation on titanium dioxide surface*. *Materials Science & Engineering C-Materials for Biological Applications* **31** (5), 1062–1067.
- Gupta, V. K., Jain, R., Agarwal, S., Nayak, A. & Shrivastava, M. 2012a *Photodegradation of hazardous dye quinoline yellow catalyzed by TiO₂*. *Journal of Colloid and Interface Science* **366** (1), 135–140.
- Gupta, V. K., Jain, R., Mittal, A., Saleh, T. A., Nayak, A., Agarwal, S. & Sikarwar, S. 2012b *Photo-catalytic degradation of toxic dye amaranth on TiO₂/UV in aqueous suspensions*. *Materials Science & Engineering C-Materials for Biological Applications* **32** (1), 12–17.
- Haupt, K. 2003 *Imprinted polymers—Tailor-made mimics of antibodies and receptors*. *Chemical Communications* **34** (2), 171–178.
- Jing, T., Wang, J., Liu, M., Zhou, Y. S., Zhou, Y. K. & Mei, S. R. 2014 *Highly effective removal of 2,4-dinitrophenolic from surface water and wastewater samples using hydrophilic molecularly imprinted polymers*. *Environmental Science and Pollution Research* **21** (2), 1153–1162.
- Le Noir, M., Lepeuple, A. S., Guieysse, B. & Mattiasson, B. 2007 *Selective removal of 17 beta-estradiol at trace concentration using a molecularly imprinted polymer*. *Water Research* **41** (12), 2825–2831.
- Liu, Y. T., Liu, R. H., Liu, C. B., Luo, S. L., Yang, L. X., Sui, F., Teng, Y. R., Yang, R. B. & Cai, Q. Y. 2010 *Enhanced photocatalysis on TiO₂ nanotube arrays modified with molecularly imprinted TiO₂ thin film*. *Journal of Hazardous Materials* **182** (1–3), 912–918.
- Martínez, J. M. L., Denis, M. F. L., Dall’Orto, V. C. & Buldain, G. Y. 2008 *Synthesis, FTIR, solid-state NMR and SEM studies of novel polyampholytes or polyelectrolytes obtained from EGDE, MAA and imidazoles*. *European Polymer Journal* **44** (2), 392–407.
- Meng, Z. H., Chen, W. & Mulchandani, A. 2005 *Removal of estrogenic pollutants from contaminated water using molecularly imprinted polymers*. *Environmental Science & Technology* **39** (22), 8958–8962.
- Piletsky, S. A., Alcock, S. & Turner, A. P. F. 2001 *Molecular imprinting: at the edge of the third millennium*. *Trends in Biotechnology* **19** (1), 9–12.
- Radjenovic, J., Petrovic, M. & Barcelo, D. 2007 *Advanced mass, spectrometric methods applied to the study of fate and removal of pharmaceuticals in wastewater treatment*. *Trends in Analytical Chemistry* **26** (11), 1132–1144.
- Saadi, I., Borisover, M., Armon, R. & Laor, Y. 2006 *Monitoring of effluent DOM biodegradation using fluorescence, UV and DOC measurements*. *Chemosphere* **63** (3), 530–539.
- Sansotera, M., Persico, F., Pirola, C., Navarrini, W., Di Michele, A. & Bianchi, C. L. 2014 *Decomposition of perfluorooctanoic*

- acid photocatalyzed by titanium dioxide: chemical modification of the catalyst surface induced by fluoride ions. *Applied Catalysis B-Environmental* **148**, 29–35.
- Su, Y. L., Xiao, Y. T., Fu, X., Deng, Y. R. & Zhang, F. B. 2009 Photocatalytic properties and electronic structures of iodine-doped TiO₂ nanotubes. *Materials Research Bulletin* **44** (12), 2169–2173.
- Sun, L. Z. & Bolton, J. R. 1996 Determination of the quantum yield for the photochemical generation of hydroxyl radicals in TiO₂ suspensions. *Journal of Physical Chemistry* **100** (10), 4127–4134.
- Tran, T. T., Li, J. Z., Feng, H., Cai, J., Yuan, L. J., Wang, N. Y. & Cai, Q. Y. 2014 Molecularly imprinted polymer modified TiO₂ nanotube arrays for photoelectrochemical determination of perfluorooctane sulfonate (PFOS). *Sensors and Actuators B-Chemical* **190**, 745–751.
- Wang, H. J., Zhou, W. H., Yin, X. F., Zhuang, Z. X., Yang, H. H. & Wang, X. R. 2006 Template synthesized molecularly imprinted polymer nanotube membranes for chemical separations. *Journal of the American Chemical Society* **128** (50), 15954–5.
- Zhang, H. Q., Yamada, H. & Tsuno, H. 2008 Removal of endocrine-disrupting chemicals during ozonation of municipal sewage with brominated byproducts control. *Environmental Science & Technology* **42** (9), 3375–3380.
- Zhang, W. L., Li, Y., Wu, Q. Y. & Hu, H. Y. 2012 Removal of endocrine-disrupting compounds, estrogenic activity, and Escherichia coliform from secondary effluents in a TiO₂-coated photocatalytic reactor. *Environmental Engineering Science* **29** (3), 195–201.
- Zhang, X. J., Chen, C., Lin, P. F., Hou, A. X., Niu, Z. B. & Wang, J. 2011 Emergency drinking water treatment during source water pollution accidents in china: origin analysis, framework and technologies. *Environmental Science & Technology* **45** (1), 161–167.
- Zhang, Z. B. & Hu, J. Y. 2008 Selective removal of estrogenic compounds by molecular imprinted polymer (MIP). *Water Research* **42** (15), 4101–4108.

First received 10 September 2015; accepted in revised form 13 June 2016. Available online 27 June 2016